International Journal of Innovative Technologies in Social Science

e-ISSN: 2544-9435

Scholarly Publisher
RS Global Sp. z O.O.
ISNI: 0000 0004 8495 2390

Dolna 17, Warsaw,
Poland 00-773
+48 226 0 227 03
editorial_office@rsglobal.pl

ARTICLE TITLE	PREDICTION OF SEISMIC INTENSITY IN URBAN AREAS. CASE STUDY OF THE CITY OF BATNA, ALGERIA
ARTICLE INFO	Kamel Belkhiri, Abdelmalek Rerboudj, Nassim Bella. (2024) Prediction of Seismic Intensity in Urban Areas. Case Study of The City of Batna, Algeria. *International Journal of Innovative Technologies in Social Science*. 4(44). doi: 10.31435/ijitss.4(44).2024.3008
DOI	https://doi.org/10.31435/ijitss.4(44).2024.3008
RECEIVED	11 October 2024
ACCEPTED	15 December 2024
PUBLISHED	19 December 2024
LICENSE	The article is licensed under a **Creative Commons Attribution 4.0 International License.**

PREDICTION OF SEISMIC INTENSITY IN URBAN AREAS. CASE STUDY OF THE CITY OF BATNA, ALGERIA

Kamel Belkhiri (*Corresponding Author)*
Earth Sciences Institute -Batna 2 University, Batna (Algeria)

Abdelmalek Rerboudj
Earth Sciences Institute -Batna 2 University, Batna (Algeria)

Nassim Bella
Earth Sciences Institute -Batna 2 University, Batna (Algeria)

ABSTRACT

Knowledge of a non-instrumental measurement is one of the most remarkable scientific assets; unfortunately, in seismology, it is considered the least predictable, but it does play an important role in assessing seismic risk. Batna, the capital of the Aurès region, is located in northeastern Algeria at an elevation of 1058 me, 435 km southeast of the capital Algiers, and is one of Algeria's five most important cities. Batna is also a highly vulnerable city due to the proliferation of dwellings that do not comply with seismic recommendations. Thus, it was classified as a low seismicity zone based solely on historical data from recent decades. Our work consists of analyzing and correlating historical and instrumental seismicity at the regional and local levels: the cataloged seismicity data for northeastern Algeria from 1856 to 2018 includes 3354 epicenters. To that end, our approach is based on three major axes: (a) seismic data analysis, (b) determination of seismic intensity attenuation for a target zone (the city of Batna), and (c) assessment of seismic hazardin terms of maximum expected intensity for a given return time. Using the distribution of GUMBEL Extreme Values (I and III), we were able to identify the reasonable maximum intensity limit for the city of Batna, which was estimated to be VII (MM) for a 100-year return period. This assessment provides critical support and a sound reference for the risk scenario to warn public authorities and citizens about the damages that may result from the occurrence of future earthquakes, allowing for the development of appropriate ORSEC plans and a strategy for managing and reducing seismic risk.

KEYWORDS

Seismicity, Maximum Intensity, Seismic Hazard, North-East Algeria, City of Batna

CITATION

Kamel Belkhiri, Abdelmalek Rerboudj, Nassim Bella. (2024) Prediction of Seismic Intensity in Urban Areas. Case Study of The City of Batna, Algeria. *International Journal of Innovative Technologies in Social Science*. 4(44). doi: 10.31435/ijitss.4(44).2024.3008

INTRODUCTION

The main reason for high casualties and property damage in earthquakes is a lack of knowledge about the seismic hazard of the considered localities, coupled with insufficient seismic resilience in current structures. Predicting seismic intensity in urban areas is critical in assessing and mitigating seismic risk (Sandi & Borcia, 2011). A variety of methods have been used to estimate buildings' seismic vulnerability, including response spectra and vulnerability indices. These methods aim to assess seismic risk based on intensity as an agitation parameter, as proposed in Italy by Slejko et al. (1998) and Albarello et al. (2002). Other studies have also been conducted based on observations of damage levels caused by previous earthquakes (Ferreira et al., 2019; Hadzima-Nyarko et al., 2017).

Our approach consists of assessing the macro-seismic intensity that may be reached in the event of future earthquakes in a target area (the city of Batna), which is still considered by the majority of its inhabitants to be

a non-seismic zone. In particular, it appears important to assess local seismic hazards made in the urban centers where most of the population, old (colonial era) and new buildings and infrastructures are concentrated, most of which have been erected in a way that does not comply with seismic regulations, and which remain the most vulnerable and fragile to degrees of seismic intensity (Hadzima-Nyarko et al., 2017).This type of information will undoubtedly contribute significantly to the protection and preservation of infrastructure, homes, and installations from seismic severity while also serving as a strategic axis in the information and awareness-raising efforts of both public authorities and citizens.

The most recent information on the spatial distribution of maximum calculated intensities (MCI) for Algeria between 1716 and 2000 is presented in the map by Boughacha et al. (2004), which makes it possible to identify the degree of maximum intensity between (VI-VII) for the area where the city of Batna is located (Fig.1). Batna area extends over an area of 85 $km^2$and is classified as a large city with a population of 349840 according to the *Direction de la Programmation et du SuiviBudgétaires*(DPSB, 2019).So far, the area has been considered to be characterized by very low seismic hazards.

In order to evaluate the soundness of this position, we first identified and characterized the seismic sources most likely to have an impact on each point of the target zone (the city of Batna) and provided a reasonable upper limit to the severity of effectsof future earthquakes in terms of macroseismic intensity. The mathematical approach to this calculation is known as probabilistic seismic hazard analysis, or PSHA,and is in line with the procedure proposed byCornell (1969). We also hope that our findings will help to improve the seismological model that is currently used in Algeria, as its scale and precision allow us to reason and rule solely in terms of the microspatial territorial dimension. These approaches are invaluable decision-support tools for raising awareness and alerting public authorities and citizens, allowing for the development and implementation of appropriate seismic risk-reduction strategies in urban planning sectors and areas.

SEISMOTECTONIC CONTEXT OF THE STUDY AREA

The Algerian coastal zone is bounded by two major orogens: The Atlas and the Telle (the entire mountainous southern edge, about 100 km wide). The Saharan Atlas chain is bordered to the south by the South Atlas front and by the Saharan platform, which was slightly (low) deformed during North Africa's Meso-Cenozoic history (Frizon de Lamotte et al., 2000). This NE-SW trending mountain range is the highest and most significant relief in Northern Algeria. According to the kinematic model assigned by global NUVEL1A (DeMets et al., 1990, 1994), displacement velocities quantified in the Maghrebids over the long term (the last 9 Ma) range from 4 mm/yr (at 0°E longitude) to 6 mm/yr (at 10°E longitude). The African and Eurasian plates are in constant, slow compressive motion (Serpelloni et al., 2007). The Algerian basin began to open in the Miocene behind the Tethys subduction, causing the AlKapeca domain (Alboran, Kabylies, Peloritain, and Calabria) to drift southeast between 30 and 15 million years ago. Folds affected the Tell and Atlas between the mid and late Miocene. At this point, the Tellian nappes were sinking into place(Gelabert et al., 2002; Maury et al., 2000). Leprêtre(2012) explained that the Algerian Atlasic system is the result of two major tectonic events. The first Atlasic phase is extended to the Maghreb scale, and the second occurs before the Kabylides collide with Africa (Benaouali-Mebarek et al., 2005). The Batna region has experienced rather complex tectonics, particularly in the northern part of the region, with dominant tectonics and Atlasic tectonics producing anticlinal and synclinal structures. The region is situated at the convergence of two major tectonic lineaments (Guemache, 2010). A Tenès-Negrine lineament, which corresponds to a large dexterous shear zone oriented N110°E to N120°E and stretches for nearly 700 km from the coast of Ténès in the north-west to Negrine in the southeast, runs between Batna and EL-Kantara. The second lineament of Sidi Ferdjani-El Kantra is suitable for an N55°E-directed celestial dropout that extends for approximately 400 km (Abacha, 2015).

The city of Batna is in a low seismicity zone situated between the Hodna Mountains and the Aurès Massif. It has witnessed earthquakes throughout its history. In the Roman period, the first earthquake occurred in 267 AD at Tazoult-Lambèse, 10 km from Batna. The Ngaous earthquake on January 17, 1885 (50 km from Batna) had a maximum epicentral intensity (VIII-MSK) and a magnitude of 5.7. The MacMahon (Ain Touta) earthquake on March 16, 1924, had a maximum intensity of IX-MSK and an instrumental magnitude of 5.6, with an epicenter 25 km from Batna. On October 2, 1970, an earthquake occurred very close to the city with an instrumental magnitude of 4.5 and an intensity of VI (MM) over Batna. Finally, on May 2, 1986, El Madher experienced an earthquake with an instrumental magnitude of 4.8 that caused a degree of intensity (V-MM) over Batna. Offeredby the national center for applied research in paraseismic engineering(CGS).

DATA COLLECTION

DISTRIBUTION OF EPICENTERS RECORDED

The data is provided by The CRAAG (Astronomy, Astrophysical, and Geophysical Research Center). This institution is Algeria's most credible source for earthquake information. It spans the northeastern part of the country, between the coordinates [5°-8.5° East and 34.5°-38° North] (Fig. 1). This seismic database contains 3354 events spanning from 1856 to 2018.

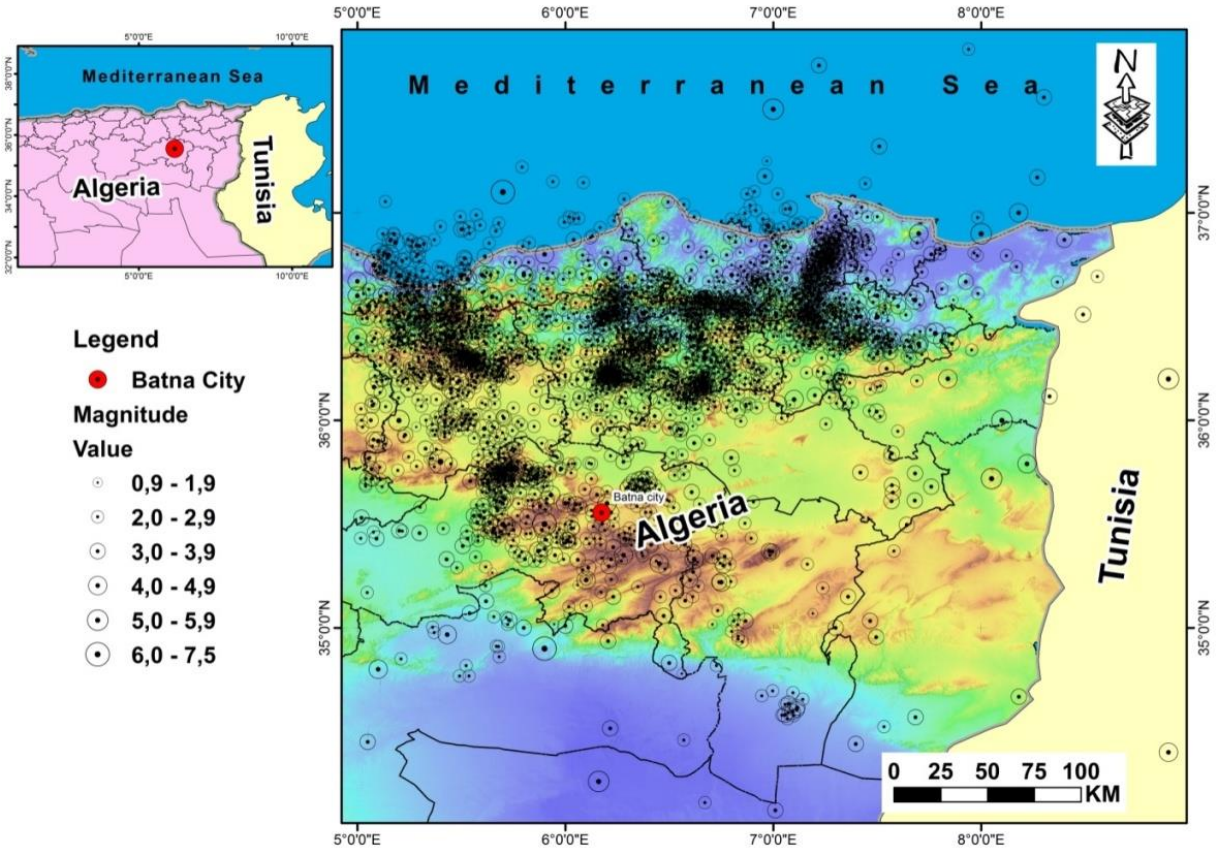

Fig. 1. Macroseismic and instrumental epicenters in northeastern Algeria (1856-2018)

These data are presented in the form of a table that describes each earthquake, including the date (Day. Month. Year) and origin time (Hour-minute-second), epicentral coordinates (Longitude, Latitude), focal depth and surface wave magnitude (Ms), and the focal depth in kilometers. The spatial distribution of all seismic events in the region (Fig. 1) provides a general representation of the source area's seismicity over the period (1856 -2018).We observe that the epicenters are more concentrated along the coast, in the Atlas Tellien. Moving southward, the frequency of seismic activity decreases dramatically. It is important to note that this region has moderate seismic activity.

The time distribution of magnitude (M) is determined by the number of measuring stations and the quality of the equipment. Fig.2 (a, b) depicts an increase in measurements. The analysis in Fig. (2a) shows a gradual improvement in seismic data records since 1991. A second increase in the number of reported events can be seen between 2001 and 2010. This is due to the improvement in the quality and number of seismographic monitoring networks in Algeria, which explains the increase in the number of earthquakes with magnitudes (0.9 - 2.9), which accounts for 82.11 % of our sample size (Fig. 2b).

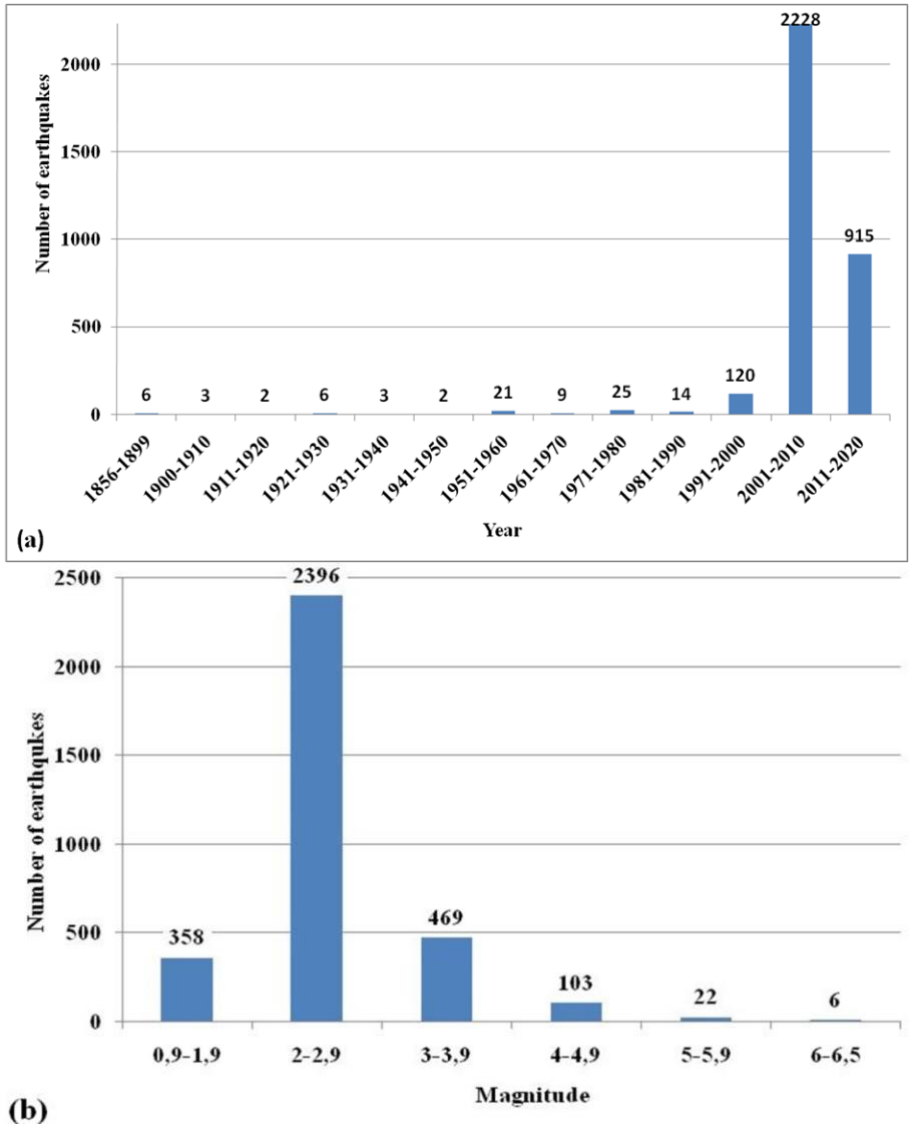

Fig. 2. Earthquake distribution, (a) magnitude by year and (b) by magnitude class (1856-2018)

METHODS

The seismic hazard at Batna was assessed by a probabilistic approach (Ameer et al., 2004) and summarized as follows:

Intensity attenuation

At first, all seismic point sources capable of producing intensities > 0 in the target area were identified. This has been achieved with the assumption that the area surrounding the city of Batna is considered homogeneous as it concerns the propagation of seismic energy from the source and that the empirical attenuation models by Shebalin(1968) and Ganse(1980)1 and 2 (Table1) hold for the study area.

Table 1. Attenuation equations for calculating epicentral intensity

Author	Relation	Intensity scale
Shebalin (1968)	$I_{(c)} = I_0 - 3{,}6 \cdot Log\ (r/h)$ (1)	MSK
Ganse1 (1980)	$LnI_c = LnI_0 - 0.10 - 0.00196\ \Delta\ - 0.076\ Ln\Delta$ (2)	MM
Ganse2 (1980)	$LnI_c = Ln(1.5M - 1.5 + 0.0477 - 0.022\Delta - 0.055Ln\Delta)$ (3)	MM

Note: I_0 is the intensity at the epicenter, Ic is the local intensity (target area), h is the focal depth (10 km), Δ is the epicentral distance $r = \sqrt{(\Delta\text{^}2 + h\text{^}2)}$ (km), and M is the instrumental magnitude.

The average of these relationships allowed us to select 1093 seismic epicenters within 200 km of the city of Batna (Fig. 3), as follows:

0 – 50 km; N=301 (3.66%) $I\_(Bmax)\hat{}obs = 6.4\ (MM)$
50 – 100 km; N=467 (26.08%) $I\_(Bmax)\hat{}obs = 4.33\ (MM)$
100 – 150 km; N=285 (42.73%) $I\_(Bmax)\hat{}obs = 3.5\ (MM)$
150 – 200 km; N=40 (27.53%) $I\_(Bmax)\hat{}obs = 2.9\ (MM)$

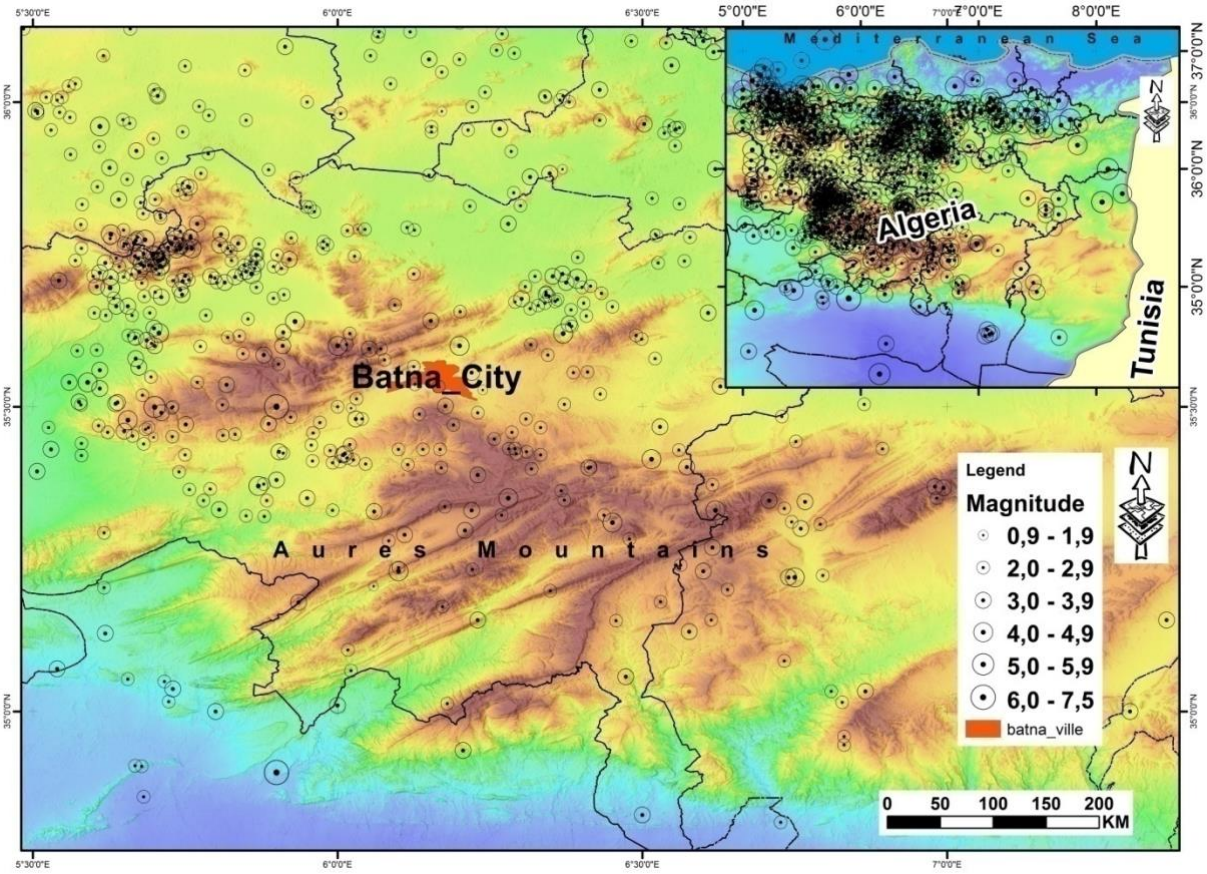

Fig. 3. Distribution of macroseismic and instrumental epicenters within a 200 km radius of the city of Batna (1856-2018)

Frequency-magnitude relationship

The magnitude of the seismic events selected in the way described above has been considered to define the frequency-magnitude relationship. Two models have been considered. The first one (Gutenberg & Richter, 1950) is in the form:

$$Log_{10}(N_c/an) = a - b.M \quad (4)$$

where, *Nc/year* is the cumulative number of events occurring per year above greater than the magnitude M. *a* and *b*respectively resulted equal to 4.65 and 0.64.

The model by Hwang and Huo (1994) was also considered in the form:

$$N(\geq M)=e^{\alpha-\beta M}.(1-e^{-\beta(M_{max}-M)})/(1-e^{-\beta(M_{max}-M_0)}) \quad (5)$$

where, $M_0 = 3$and $M_{max}$is the maximum credible earthquake in the area, α and β in (4). In this case, the values for the relevant parameters were $M_{max} = 6.5$ (Fig. 5),

$\alpha = a.\ Ln(10) = 10.70$ (6)
$\beta = b.\ Ln(10) = 1.47$ (7)
$M_{max} = 6.5,\ M0 = 3$

$$N(\geq M) = e^{10.7-1.47M}.(1 - e^{-1.47(6.5-M)})/(1 - e^{-1.47(6.5-3)})$$

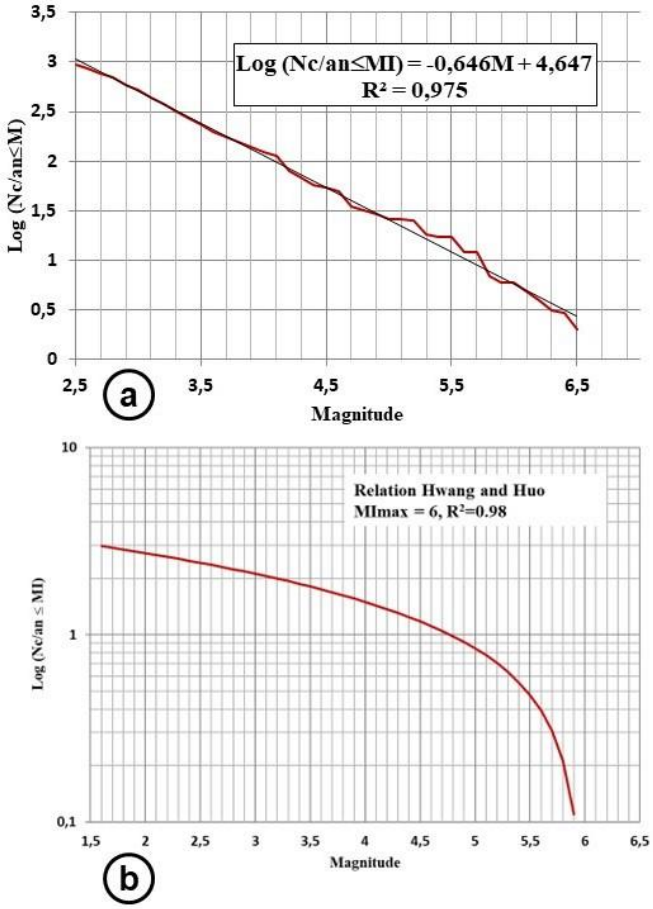

Fig. 4. Relation frequency magnitude for the period 1856 – 2018
(a) By Gutenberg and Richter, (b) By Hwang and Huo

Determination of extreme values by the GUMBEL I and III distributions:

It is assumed that extreme magnitude values per year follow a GUMBEL distribution (Ameer et al., 2004). The GUMBEL distribution (I) is the cumulative function of Burton (1979):

$$G_{(M)} = \exp\ [-\exp\ [(\beta\ \ (M\ -\ u))]] \quad (8)$$

where, β and μ are empirical coefficients. To compute these coefficients, the series of maximum magnitudes of earthquakesthat occurred each year is considered. These *N* values are then arranged in increasing order, and to each *Mi* value in the ordered series, rank i is assigned. Then,an empirical Hazen distribution of $G\_((M))\text{^}I\ (Mi)$ is defined as:

$$G_{(M)}=(i-0,5)/N \quad (9)$$

This empirical frequency distribution is fitted by the model in equation (8), and the respective $\beta$and u values are determined in the case that an upper bound is expected to exist for the magnitude M of earthquakes in the area. A different fitting model is considered in the form of the GUMBEL distribution (III) can be considered in the form:

$$G\ III(M) = e\{-[(w - M)/(w - u)]^k\} \quad (10)$$

Where the two parameters*w*, *U*, and *k* respectively represent the upper limit of the variate *M*, *the* greatest characteristic value, and a shape parameter (Jaiswal et al., 2002; Mohammadi & Bayrak, 2016; Tsapanos et al., 2014); (Fig.5).

Let *Mi* (with *i* =1, 2, 3, …, *n*) be the observed earthquake magnitudes in the source zone from 1856 - 2018.The average return time *T* of an event is defined as the reciprocal of the number of times the event occurred

$$\mathrm{T} = 1/(1 - \mathrm{G}^{\mathrm{I}}_{(\mathrm{M})}(\mathrm{Mi}))) \quad (11)$$

This average allows for the estimation of the maximum magnitude corresponding to the average return time *T*.

RESULTS

Intensity attenuation

The earthquake that occurred on March 16, 1924, had its epicenter located at Lat N. 35 - 500; Long. °E 05 - 900. The instrumental magnitude was *M = 5.6*, the epicentral intensity was I_0 *= IX (MM)*, and the epicentral distance was Δ *= 25.50 Km* from the city of Batna. These findings allowed us to determine the maximum intensity observed $I\_(BMax)\hat{}Obs = 6.4\ (MM)$ in the target area.

Frequency-magnitude relationship

Analysis of the data presented in Figure 4a, frequency-magnitude relationship, Gutenberg Richter (1950). Shows that the regression line fits the data well, except for high amplitudes (Ml≥ 5).

Figure 4b, frequency-amplitude relationship, Gutenberg Richter (1950)and Hwang and Huo (1994). Express the extent of observation of the cataloged values capped at the magnitude between (6) of the source zones and the target zone.

Determination of extreme values using GUMBEL I and III distributions

The Gumbel I and III methods were used with earthquakes created specifically for our site (the city of Batna). The earthquakes (historical or instrumental), epicentral intensity (I_0), and intensity (*IB*) in the target site (we used the attenuation relationships of epicentral intensity (I_0) with distances established by Shebalin(1968) and Ganse (1980), as shown in table (1), produced between 1856 and 2018. Figure 5 shows the obtained results.

Table 3 displays magnitudes, epicentral intensities (I_0), and intensities at the target site (Batna) (*IB*) as a function of the return period. The maximum likelihood estimates of the Gumbel distribution over 100 years are very similar to those of GUTENBERG RICHTER and Hwang &Huo (Intensity of Batna city (IB) estimates VIII (MM) for 475 years of the return period). However, the estimates for the 475 years are one degree higher than those by Gutenberg Richter. As a result, an earthquake with an epicentral magnitude of 7.4 (Richter) is defined as one capable of generating large forces in the target area.

Table 2. Central seismic magnitude and intensity parameters for the city of Batna (1856-2018)

	Magnitude	**Epicentral Intensity**	**Shebalin**	**Ganse(1-2)**	**Ganse (2-2)**	**Batna city**
Average	3.07	4.33	1.32	2.99	0.58	1.63
Median	3	4.11	1.08	2.83	0.92	1.46
Mode	2.8	3.98	4.2	4.99	0.61	3.27
Max. value	6.5	8.8	7.31	7.3	3.94	6.18
Standard deviation	0.71	0.94	1.031	0.60	0.48	0.66

Table 3. Magnitude (M) epicentral intensity of Batna (local) obtained by GUMBEL I and GUMBEL III methods

	GUMBEL (G-I)			GUMBEL (G-III)		
Return period	**Epicenter magnitude**	**Epicenter intensity**	**Intensity of Batna city**	**Epicenter magnitude**	**Epicenter intensity**	**Intensity of Batna city**
50	6.81	8.70	5.70	6.50	8.01	6.34
100	7.15	9.04	6.63	6.83	8.81	6.97
200	7.50	9.50	7.56	7.12	9.46	7.60
475	8.10	10.02	8.70	7.46	10.22	8.25
	a= 2.80 b = 0.70 R^2=0.98	a= 3.90 b= 0.73 R^2=0.98	a=0.51 b=1.33 R^2=0.98	W=6.50 U=5.80 K=3.29	W=9.00 U=3.60 K=1.96	W=7.00 U=3.70 K=1.72

DISCUSSION

According to Gutenberg and Richter (1950) and Hwang and Huo (1994), the magnitude in northeastern Algeria [5°- 8.5° E and 34.5°-38° N] is approximately 6.5 (Richter), while in the target zone, which includes the town of Batna, it is 6 (Richter). These findings are nearly identical to those obtained using GUMBEL's law (I-III) over a 100-year return period. M_{max} = *6.83* (Richter); I_{max} = *VI-VII* (MM); see Table 3. As a result, GUMBEL's law III suggests that for a 475-year return period, the magnitude M_{max} = *7.46* (Richter) for the source zone be limited, resulting in a maximum intensity I_{max} = *VIII* (MM) for the target zone. The results of this study are comparable to those of Peláez et al.(2005) (M_{max} = *6.8*) and Aoudiaet al. (2000) (M_{max} = *6.1*) in the Aures-Nememcha zone for the same return period (100 years). These findings provide strong support for our approach. It also suggests that the environment is more uniform and capable of producing large earthquakes. For example, the Biskra-Aures earthquake of November 16, 1869 (34.90°N; 5.90°E) had an intensity of IX (MM) (Yelles-Chaouche et al., 2017) and was the strongest earthquake ever recorded, killing 30 people in the region. Thus, seismic activity exists in this area, albeit at a low frequency. Consequently, this method provides a sound basis for drawing up an ORSEC emergency response plan.

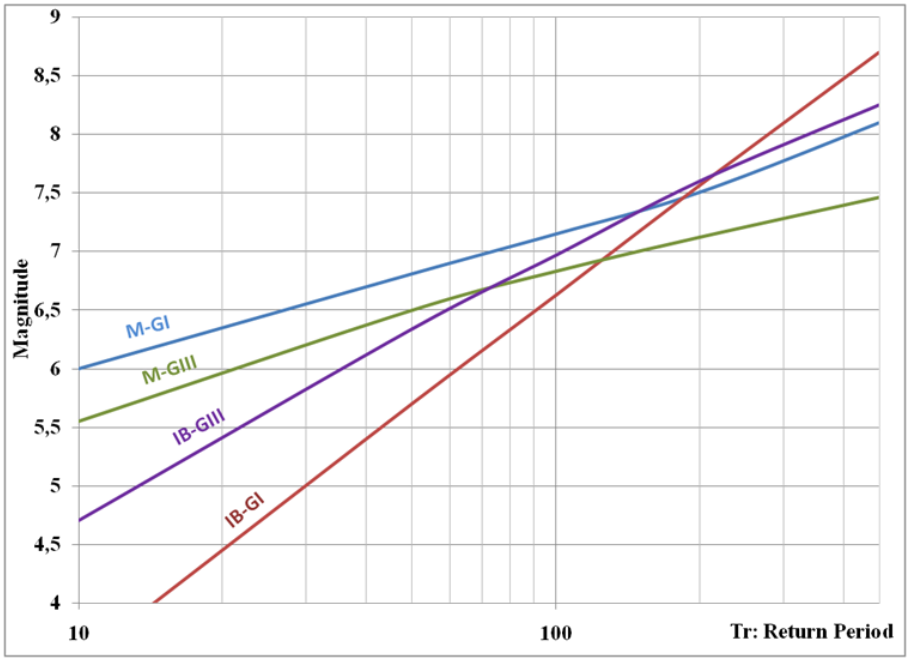

Fig. 5. Graphical representation of the distributions of extreme GUMBEL values (G.I and G.III) for the magnitude(M) of the source zone and the intensity(I) of the city of Batna (target zone), instrumental and historical seismic data (1856-2018)

CONCLUSIONS

This study presented a simple method for conducting quick and preliminary surveys in regions with limited seismic data. The method combines the frequency-magnitude law (Gutenberg & Richter, 1950; Hwang & Huo, 1994) with the parameters of GUMBEL's asymptotic distributions of type I and type III using seismic data from North-east Algeria from 1856 to 2018. The conventional approach is based on the frequency-amplitude relationship, which provides ceiling limits on amplitude that do not exceed the sample threshold value. As a result, the method is not appropriate for modeling rare and large earthquakes. These two relations continue to be extremely useful in determining the degree of observation of the maximum magnitude of the source and target areas.

The extreme values for the city of Batna have been predicted using the maximum observed intensity (I_{max} =VIII) over a 475-year return period. This maximum observed intensity can be regarded as a very useful seismic hazard parameter because it provides us with immediate downstream information on the extent of the expected damage in the event of a similar earthquake in the study area, which has fewer microseismic recordings. In light of these findings, we are fully motivated to create a numerical model that can quickly and reliably calculate seismic intensity at any point in the target area.

REFERENCES

1. Abacha, I. (2015). *Étude de la sismicité de la région Nord-Est de l'Algérie*. Université Ferhat Abbas-Sétif.
2. Albarello, D., & Mucciarelli, M. (2002). Seismic Hazard Estimates Using Ill-defined Macroseismic Data at Site. *Pure and Applied Geophysics*, *159*(6), 1289–1304. https://doi.org/10.1007/s00024-002-8682-2
3. Ameer, A. S., Sharma, M. L., Wason, H. R., & Alsinawi, S. A. (2004). Seismic hazard characterization and risk evaluation using Gumbel's method of extremes (G1 and G3) and GR formula for Iraq. *13th World Conference on Earthquake Engineering, Vancouver, B.C., Canada August 1-6, 2004 Paper No. 2898*. https://www.researchgate.net/profile/Mukat-Sharma/publication/267768010_seismic_hazard_characterization_and_risk_evaluation_using_gumbel's_method_of_extremes_g1_and_g3_and_gr_formula_for_iraq/links/584db93008aeb989252643a8/seismic-hazard-characterization-and-risk-evaluation-using-gumbels-method-of-extremes-g1-and-g3-and-g-r-formula-for-iraq.pdf
4. Aoudia, A., Vaccari, F., Suhadolc, P., & Meghraoui, M. (2000). Seismogenic potential and earthquake hazard assessment in the Tell Atlas of Algeria. *J Seismol*, *4*(1), 79–98. https://doi.org/https://doi.org/10.1023/A:1009848714019
5. Benaouali-Mebarek, N., Frizon de Lamotte, D., Roca, E., Bracene, R., Faure, J.-L., Sassi, W., & Roure, F. (2005). Post-Cretaceous kinematics of the Atlas and Tell systems in central Algeria: Early foreland folding and subduction-related deformation. *Comptes Rendus. Géoscience*, *338*(1–2), 115–125. https://doi.org/10.1016/j.crte.2005.11.005
6. Boughacha, M. S., Ouyed, M., Ayadi, A., & Benhallou, H. (2004). Seismicity and seismic hazard mapping of northern Algeria: Map of Maximum Calculated Intensities (MCI). *Journal of Seismology*, *8*(1), 1–10. https://doi.org/10.1023/B:JOSE.0000009513.11031.43
7. Burton, P. W. (1979). Seismic risk in southern Europe through to India examined using Gumbel's third distribution of extreme values. *Geophysical Journal International*, *59*(2), 249–280. https://doi.org/10.1111/j.1365-246X.1979.tb06766.x
8. Cornell, C. A. (1969). A Probability-Based Structural Code. *ACI Journal Proceedings*, *66*(12). https://doi.org/10.14359/7446
9. DeMets, C., Gordon, R. G., Argus, D. F., & Stein, S. (1990). Current plate motions. *Geophysical Journal International*, *101*(2), 425–478. https://doi.org/10.1111/j.1365-246X.1990.tb06579.x
10. DeMets, C., Gordon, R. G., Argus, D. F., & Stein, S. (1994). Effect of recent revisions to the geomagnetic reversal time scale on estimates of current plate motions. *Geophysical Research Letters*, *21*(20), 2191–2194. https://doi.org/10.1029/94GL02118
11. Ferreira, T. M., Mendes, N., & Silva, R. (2019). Multiscale Seismic Vulnerability Assessment and Retrofit of Existing Masonry Buildings. *Buildings*, *9*(4), 91. https://doi.org/10.3390/buildings9040091
12. Frizon de Lamotte, D., Saint Bezar, B., Bracène, R., & Mercier, E. (2000). The two main steps of the Atlas building and geodynamics of the western Mediterranean. *Tectonics*, *19*(4), 740–761. https://doi.org/10.1029/2000TC900003
13. Ganse, R. A. (1980). Expected-Intensity Searches and Attenuation Coefficients for China, Turkey and Yugoslavia. *Seismological Research Letters*, *51*(2), 26–27. https://doi.org/10.1785/gssrl.51.2.26
14. Gelabert, B., Sàbat, F., & Rodríguez-Perea, A. (2002). A new proposal for the late Cenozoic geodynamic evolution of the western Mediterranean. *Terra Nova*, *14*(2), 93–100. https://doi.org/10.1046/j.1365-3121.2002.00392.x
15. Guemache, M. A. (2010). *Évolution géodynamique des bassins sismogènes de l'Algérois (Algérie) : Approche pluridisciplinaire (méthodes géologiques et géophysiques*. université de l'USTHB.
16. Gutenberg, B., & Richter, C. F. (1950). Seismicity of the Earth and associated phenomena. *MAUSAM*, *1*(2), 174–176. https://doi.org/10.54302/mausam.v1i2.4568

17. Hadzima-Nyarko, M., Mišetić, V., & Morić, D. (2017). Seismic vulnerability assessment of an old historical masonry building in Osijek, Croatia, using Damage Index. *Journal of Cultural Heritage*, *28*, 140–150. https://doi.org/10.1016/j.culher.2017.05.012
18. Hwang, H. H. M., & Huo, J.-R. (1994). Generation of hazard-consistent fragility curves. *Soil Dynamics and Earthquake Engineering*, *13*(5), 345–354. https://doi.org/10.1016/0267-7261(94)90025-6
19. Jaiswal, K., Gupta, S., & Sinha, R. (2002). Estimation of maximum magnitude earthquakes in Peninsular India using extreme value statistics. *12th Symposium on Earthquake Engineering, IIT Roorkee; India*, 313–323. https://www.researchgate.net/profile/Sushil-Gupta-14/publication/328277795_estimation_of_maximum_magnitude_earthquakes_in_peninsular_india_using_extreme_value_statistics/links/5bc38f11a6fdcc2c91fbec08/estimation-of-maximum-magnitude-earthquakes-in-peninsular-india-using-extreme-value-statistics.pdf
20. Leprêtre, A. (2012). *Contraintes par imagerie sismique pénétrante sur l'évolution d'une marge Cénozoïque réactivée en compression (cas de la marge algérienne, secteur de Tipaza)*. Université de Bretagne occidentale - Brest.
21. Maury, R. C., Fourcade, S., Coulon, C., El Azzouzi, M., Bellon, H., Coutelle, A., Ouabadi, A., Semroud, B., Megartsi, M., Cotten, J., Belanteur, O., Louni-Hacini, A., Piqué, A., Capdevila, R., Hernandez, J., & Réhault, J.-P. (2000). Post-collisional Neogene magmatism of the Mediterranean Maghreb margin: a consequence of slab breakoff. *Comptes Rendus de l'Académie Des Sciences - Series IIA - Earth and Planetary Science*, *331*(3), 159–173. https://doi.org/10.1016/S1251-8050(00)01406-3
22. Mohammadi, H., & Bayrak, Y. (2016). Regional Variations of the ω-upper Bound Magnitude of GIII Distribution in the Iranian Plateau. *Acta Geophysica*, *64*(4), 1004–1033. https://doi.org/10.1515/acgeo-2016-0038
23. Peláez, J. A., Hamdache, M., & Casado, C. L. (2005). Updating the Probabilistic Seismic Hazard Values of Northern Algeria with the 21 May 2003 M 6.8 Algiers Earthquake Included. *Pure and Applied Geophysics*, *162*(11), 2163–2177. https://doi.org/10.1007/s00024-005-2708-5
24. Sandi, H., & Borcia, I. S. (2011). Une raison suffisante pour redéfinir l'intensité sismique : éviter des erreurs dans l'estimation de l'aléa sismique. *CONSTRUCŢII*, *2*(January 2011), 65–76.
25. Serpelloni, E., Vannucci, G., Pondrelli, S., Argnani, A., Casula, G., Anzidei, M., Baldi, P., & Gasperini, P. (2007). Kinematics of the Western Africa-Eurasia plate boundary from focal mechanisms and GPS data. *Geophysical Journal International*, *169*(3), 1180–1200. https://doi.org/10.1111/j.1365-246X.2007.03367.x
26. Shebalin, N. V. (1968). Methods of application of seismic engineering data for regional seismity. *Regional Seismity in the USSR, Nauka Publ. House, Moscow*, 95–111.
27. Slejko, D., Peruzza, L., & Rebez, A. (1998). Seismic hazard maps of Italy. *Annali Di Geofisica*, *41*(2), 183–214.
28. Tsapanos, T. M., Bayrak, Y., Cinar, H., Koravos, G. C., Bayrak, E., Kalogirou, E. E., Tsapanou, A. V., & Vougiouka, G. E. (2014). Analysis of largest earthquakes in Turkey and its vicinity by application of the Gumbel III distribution. *Acta Geophysica*, *62*(1), 59–82. https://doi.org/10.2478/s11600-013-0155-8
29. Yelles-Chaouche, A., Kherroubi, A., & Beldjoudi, H. (2017). The large Algerian earthquakes (267 A.D.-2017). *Física de La Tierra*, *29*. https://doi.org/10.5209/FITE.57617